Title
Determination of optimal view angles for quantitative facial image analysis

Journal
Journal of Biomedical Optics, 10(2)

ISSN
1083-3668

Authors
Jung, Byungjo
Choi, Bernard
Shin, Yongjin
et al.

Publication Date
2005

DOI
10.1117/1.1895987

Determination of optimal view angles for quantitative facial image analysis

Byungjo Jung
Yonsei University,
Department of Biomedical Engineering
Korea, 220-710

Bernard Choi
University of California, Irvine
Beckman Laser Institute
1002 Health Sciences Road East
Irvine, California 92612-1475
E-mail: bjung@laser.bli.uci.edu

Yongjin Shin
University of California, Irvine
Beckman Laser Institute
1002 Health Sciences Road East
Irvine, California 92612-1475
and
Chosun University
Department of Physics
Gwangju, 501-759, Korea

Anthony J. Durkin
J. Stuart Nelson
University of California, Irvine
Beckman Laser Institute
1002 Health Sciences Road East
Irvine, California 92612-1475

Abstract. In quantitative evaluation of facial skin chromophore content using color imaging, several factors such as view angle and facial curvature affect the accuracy of measured values. To determine the influence of view angle and facial curvature on the accuracy of quantitative image analysis, we acquire cross-polarized diffuse reflectance color images of a white-patched mannequin head model and human subjects while varying the angular position of the head with respect to the image acquisition system. With the mannequin head model, the coefficient of variance (CV) is determined to specify an optimal view angle resulting in a relatively uniform light distribution on the region of interest (ROI). Our results indicate that view angle and facial curvature influence the accuracy of the recorded color information and quantitative image analysis. Moreover, there exists an optimal view angle that minimizes the artifacts in color determination resulting from facial curvature. In a specific ROI, the CV is less in smaller regions than in larger regions, and in relatively flat regions. In clinical application, our results suggest that view angle affects the quantitative assessment of port wine stain (PWS) skin erythema, emphasizing the importance of using the optimal view angle to minimize artifacts caused by nonuniform light distribution on the ROI. From these results, we propose that optimal view angles can be identified using the mannequin head model to image specific regions of interest on the face of human subjects.
[DOI: 10.1117/1.1895987]

Keywords: erythema; facial imaging; port wine stain; digital imaging; reflectance imaging.

Paper 04046 received Mar. 26, 2004; revised manuscript received Aug. 12, 2004; accepted for publication Aug. 17, 2004; published online Apr. 29, 2005.

1 Introduction

Assessment of skin chromophore (melanin and hemoglobin) content is important to identify the presence of cutaneous pathology or to monitor patient response to therapeutic intervention of skin disease. Quantitative point-measurement devices, such as reflectance spectrophotometers and tristimulus colorimeters, have been employed to estimate the content of melanin and hemoglobin in human skin.[1–5] The clinical usefulness of spectrophotometers and colorimeters is limited by practical considerations such as small test area, potential skin blanching due to probe contact, poor spatial resolution (measurements are typically resolved on a spatial scale equivalent to the dimensions of the probe head), and difficulty in relocating the probe to the same site over the longitudinal course of therapy, which may have a duration of years. Another technique under investigation is digital photography,[6–10] which addresses several limitations of spectrophotometers and colorimeters.[11] Digital photography techniques can be used to characterize a large skin area in a noncontact geometry with relatively high spatial resolution, addressing such limitations of point-measurement devices.

To maximize the ability of digital photography to compare quantitatively skin chromophore content measurements at different patient visits, it is necessary to control the imaging environment. In a previous study, we described a cross-polarized diffuse reflectance color imaging system to obtain subsurface skin color information and a head-positioning device that enabled acquisition of facial images in a reproducible fashion at a fixed distance from the illumination source.[12] An advantage of our cross-polarized diffuse reflectance imaging system is that polarization optics enables us to reject skin surface glare.[13] When the polarized light is incident on skin, ~4% of the incident light is specularly reflected at the skin surface due to the refractive index mismatch between human skin and air and ~3% of the incident light is reflected from the initial skin layer, retaining the linear polarization of the incident light. The remaining 93% of the incident light penetrates into the deep skin, and is depolarized by multiple scattering events. Eventually, about half of the depolarized light

Address all correspondence to Byungio Jung, University of California, Irvine, 1002 Health Sciences Road East, Irvine, CA 92612-1475. Fax: 949-824-6969; E-mail: bjung@laser.bli.uci.edu

1083-3668/2005/$22.00 © 2005 SPIE

that consists of light that is parallel and perpendicular to the incident polarized light is backscattered to the skin surface. The specularly reflected light is the source of glare at the skin surface, which impairs observation of skin color information provided by light scattered and absorbed from subsurface structures. Since specularly reflected light is in the same polarization state as incident polarized light, a polarizer located between the subject and the detector having its axis perpendicular to the incident light polarizer can be used to remove specular reflectance. The resulting images primarily contain subsurface information related to skin structure and chromophore content.

Also described in the previous study was an image analysis method to characterize quantitatively melanin and hemoglobin content of hypervascular port wine stain (PWS) birthmarks in human skin using L^* and a^* values, respectively, from the Commission Internationale de l'Eclairage (CIE) $L^*a^*b^*$ color space. Since most PWS lesions occur on the face,[14] it is necessary to determine the influence of view angle of the camera system and facial surface curvature on the color values derived from the images. To examine the effects of such variables on quantitative image analysis, we conducted experiments using a mannequin head model and a PWS human subject. We present a procedure that minimizes the effects of view angle and facial curvature on the accuracy of quantitative analysis of the erythema (i.e., index of hemoglobin content) in human skin.

2 Materials and Methods

2.1 *Imaging System and Image Acquisition*

The system employed for these investigations is identical to that described previously.[12] Briefly, the imaging system [Fig. 1(a)] is based on a Minolta DiMAGE 7 digital camera. Camera output was displayed on a 9-in. color monitor. The system incorporates an ac adapter powered ring flash for consistent uniform illumination. Cross-polarized optics are used to remove surface glare, which corrupts subsurface skin color measurement. Using a Kodak gray card (E152 7795, Tiffen, Rochester, New York), the white balance and exposure of the digital camera were manually adjusted to set the chromatic ratio at red $(R)=128$, green $(G)=128$, and blue $(B)=128$. The optimized camera parameters were ISO 200, aperture size $F/8$, shutter speed 1/60 s, and flash intensity level of 1/2. To eliminate artifacts induced by environmental lighting, digital images were acquired in a darkened room.

To ensure that test sites on the face were positioned in a reproducible manner, a custom head-positioning device [Fig. 1(b)] was constructed and placed within the working distance (50 cm) of the ring flash, resulting in uniform illumination. The view angle for facial imaging was selected by rotating the head-positioning device, as indicated by the bidirectional arrow in Fig. 2 and defined as the angle between the optical axis of the imaging system and the medial facial plane. The optimal view angle was defined as the view angle that minimized nonuniform illumination on the facial region of interest.

2.2 *Calculation of L* and a**

Using the algorithm for color space conversion,[15,16] the device-dependent RGB (red, green, and blue) color images were converted into the device-independent CIE $L^*a^*b^*$ color images to determine objectively skin color. In the CIE $L^*a^*b^*$ color space, the reflected light intensity was quantified[17] as L^* and erythema as a^*. Higher L^* and a^* values are indicative of higher reflectivity and erythema values, respectively. For the color space conversion, the tristimulus X, Y, and Z images of the sample (skin) and calibration reference were first calculated from respective RGB color images using the D_{65} (average daylight illumination at a standardized blackbody temperature of 6500 K) conversion matrix[16] [Eq. (1)]. As a calibration reference, RGB values for a 99% diffuse reflectance standard (Model SRT-99-100, Labsphere, North Sutton, New Hampshire) with a uniform flat surface of 30 cm^2 were measured.

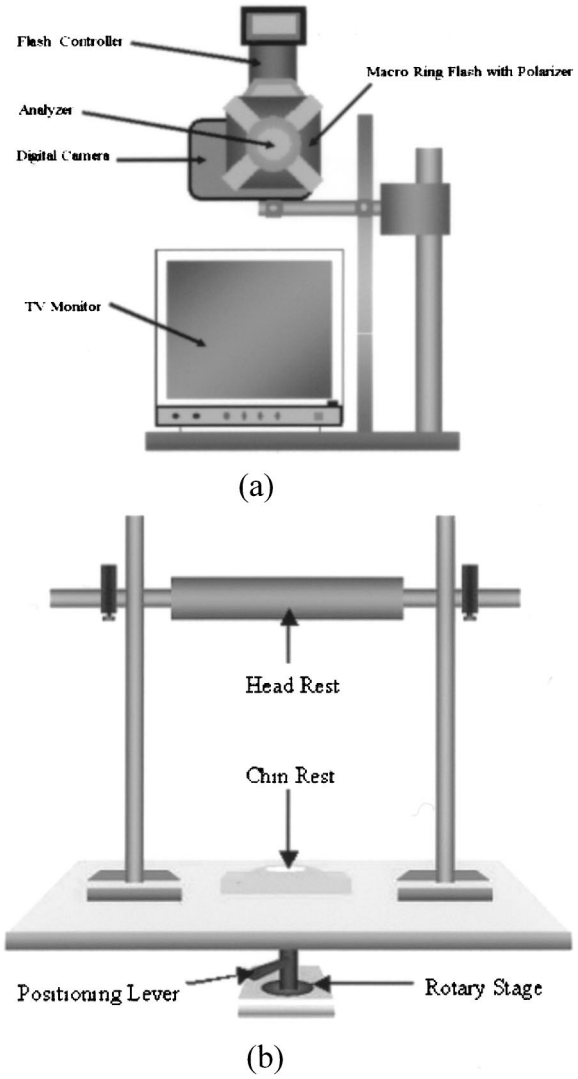

Fig. 1 (a) Diagram of the cross-polarized diffuse reflectance imaging system and (b) of the head positioning device used to standardize images obtained from each subject.

$$\begin{bmatrix} X \\ Y \\ Z \end{bmatrix} = \begin{bmatrix} 0.412453 & 0.357580 & 0.180423 \\ 0.212627 & 0.715160 & 0.072169 \\ 0.019334 & 0.119193 & 0.950227 \end{bmatrix} \begin{bmatrix} R \\ G \\ B \end{bmatrix}. \quad (1)$$

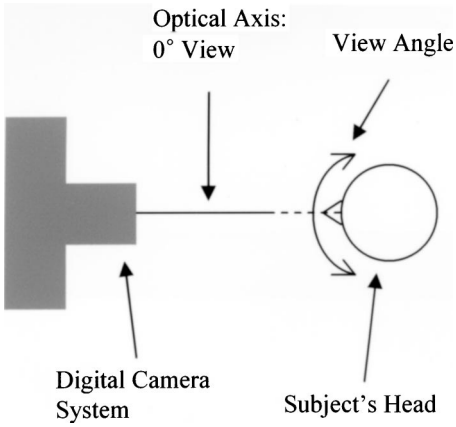

Fig. 2 Schematic diagram for facial image acquisition. View angles, defined as the angle between the optical axis of the imaging system and medial facial plane, were selected by adjusting the rotation of the head-positioning device.

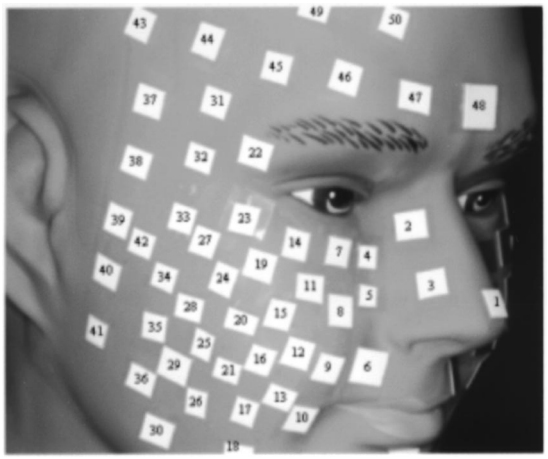

Fig. 3 Mannequin head model used to study the uniformity of the light distribution. Fifty white patches were positioned on the entire right side-face of the mannequin head model. This image was acquired at a view angle of 45 deg.

Tristimulus images for the skin (X,Y,Z) and calibration reference (X_n,Y_n,Z_n) were utilized to calculate $L^*a^*b^*$ color images using the following equations:

$$L^* = \begin{cases} 116(Y/Y_n)^{1/3} - 16 & \text{for } Y/Y_n > 0.008856 \\ 903.3(Y/Y_n) & \text{otherwise} \end{cases},$$

$$a^* = 500[f(X/X_n) - f(Y/Y_n)], \tag{2}$$

$$b^* = 200[f(Y/Y_n) - f(Z/Z_n)],$$

where

$$f(t) = \begin{cases} t^{1/3} & \text{for } t > 0.008856 \\ 7.787t + 16/116 & \text{otherwise} \end{cases}.$$

2.3 *Uniformity of Light Distribution*

Ideally, light incident on the target area should be uniformly distributed for accurate quantitative image analysis. To investigate the influence of view angle on the uniformity of incident light distribution, the 99% diffuse reflectance standard was placed in the head-positioning device. Cross-polarized diffuse reflectance images were acquired at view angles of 0 and 35 deg, which were assumed to be optimal and suboptimal angles, respectively. The L^* images for both angles were computed from the cross-polarized diffuse reflectance images.

2.4 *Mannequin Head Model*

The uniformity of light distribution due to facial curvature was studied with a physical mannequin head model, assuming that the mannequin face is representative of the shape of the human face. Fifty white patches (of 1-cm^2 area each) were removed from a Kodak gray card and positioned on the entire right-side face of the mannequin head model (Fig. 3).

2.5 *Determination of Optimal View Angle*

The mannequin head model with attached white patches was placed in the head-positioning device and cross-polarized diffuse reflectance images were obtained at multiple view angles varying between 0 and 90 deg, inclusive, in increments of 10 deg. From each image, L^* values of the patches were computed using Eqs. (1) and (2). The optimal view angle was determined based on the average L^* value and coefficient of variation (CV) of the selected white patches. Mean (μ) and standard deviation (σ) values of L^* from different subsets of patches were computed and the CV calculated as follows:

$$\mathrm{CV}(\%) = [\sigma/\mu] \times 100. \tag{3}$$

A lower CV indicates a lower dispersion in L^* over the subset of patches and, therefore, a more uniform incident light distribution. Statistical analysis was performed using SPSS software (Version 8, SPSS Inc, Chicago, Illinois).

2.6 *Determination of Optimal View Angle for Clinical Imaging*

To simulate a PWS lesion, 16 red color patches (of 1-cm^2 area each) from a Macbeth color checker (GretagMacbeth, New Windor, New York) with 24 different color patches were placed on the left-side face of the mannequin model and on a human subject with normal skin (Fig. 4). This color checker is used as a standard in evaluation of color measurement devices.[16] Every effort was made to place the patches on identical locations on both the model and the subject. From images of white patches placed at corresponding locations on the contralateral side of the model (i.e., patches 2 to 9, 11, 12, 14 to 16, 19, 20, 23, 24, and 27 in Fig. 3), the optimal view angle to image the entire red-patched region was determined from calculated CV values as described above. Using this optimal view angle, images of the red patches on both the model and subject were acquired and a^* values were determined.

The clinical relevance of view angle was investigated on a PWS patient receiving laser treatment at Beckman Laser Institute. Images were acquired at two different suboptimal view angles and, then, the respective a^* images were compared to demonstrate the importance of view angle for quantitative image analysis. Three consecutive cross-polarized diffuse reflectance color images were acquired at the optimal view angle for the PWS lesion over an 8-week period. Qualitative assess-

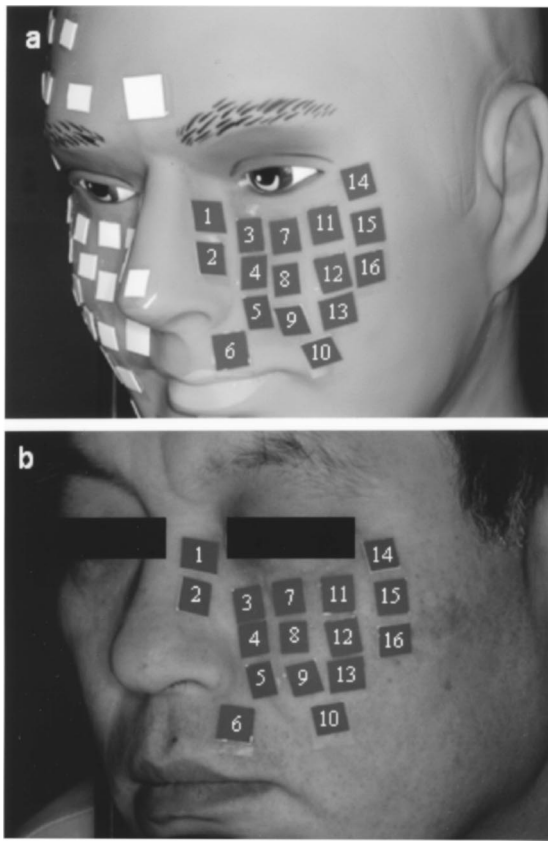

Fig. 4 To simulate a PWS birthmark, red-patches were positioned on (a) the mannequin head model and (b) a human subject. Sixteen red patches were placed at similar locations on both the mannequin head model and the human subject. Cross-polarized diffuse reflectance images were acquired at the optimal view angle of 35 deg.

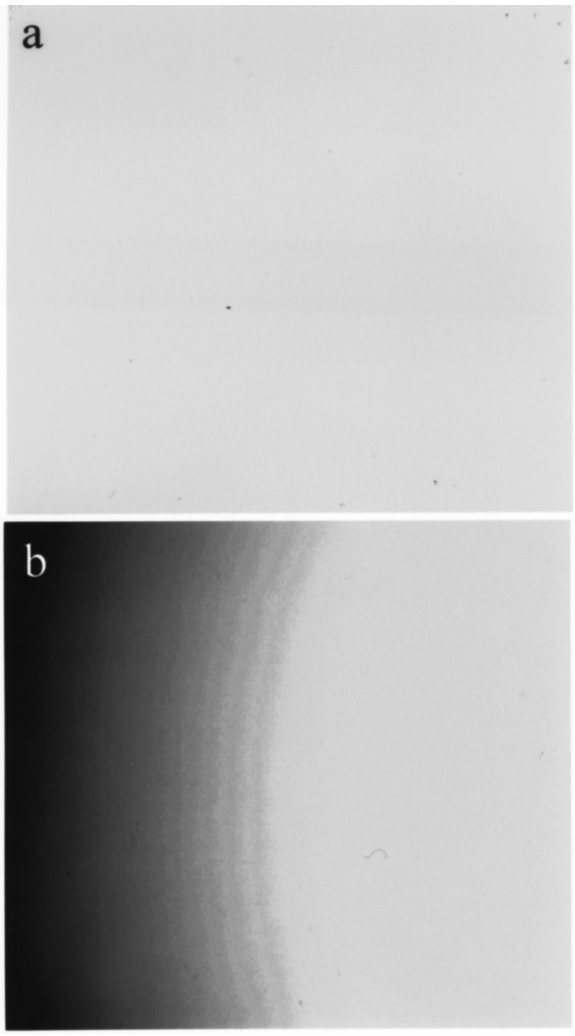

Fig. 5 Light distribution on the 99% diffuse reflectance standard at view angles of (a) 0 and (b) 35 deg. Image contrast was adjusted to enhance visualization of the light distribution.

ment was performed by comparing PWS skin color changes in consecutive images. For quantitative assessment of changes in PWS erythema, a^* images were computed from the corresponding cross-polarized diffuse reflectance images.

3 Results

3.1 *Optimized Imaging System Provides a Uniform Light Distribution on a Flat Surface*

Using the selected camera parameters, a uniform light distribution on the 99% diffuse reflectance standard was obtained at a view angle of 0 deg [Fig. 5(a)]. At a view angle of 35 deg, the resultant light distribution was nonuniform [Fig. 5(b)]. To test system stability, images of the diffuse reflectance standard were acquired at a view angle of 0 deg on 5 separate days. RGB values ($\mu \pm \sigma$) were 250 ± 1.3, 252 ± 1.7, and 251 ± 1.2, respectively, demonstrating the stability of our imaging system.

3.2 *Optimal View Angle Depends on the Region of Interest*

To simulate different regions of interests (ROIs) on the face, optimal view angles were determined for various subsets of the 50 white patches placed on the mannequin head model. Figure 6 illustrates the dependence of L^* values on view angle for a ROI covering primarily the front side of the face (i.e., patches 2 to 21 in Fig. 3). The CV is a minimum (1.2%) at a view angle of 40 deg, suggesting that this is the optimal view angle. Based on the results shown in Table 1, the optimal view angle varies and should be determined based on the ROI under study.

Use of the red patches to simulate a PWS lesion resulted in similar CV results for both the mannequin head model and human subject with normal skin. From the white-patched mannequin head model data shown in Fig. 7, the optimal view angle for the red patched region was determined to be 35 deg (CV 0.4%). At this optimal view angle, the mean a^* values of the red patches on the mannequin model and human subject with normal skin were 37.47 ± 0.63 (CV 1.6%) and 40.64 ± 0.78 (CV 1.9%), respectively. From the image of the red patches at a 0-deg view angle, the mean a^* value was 38.98 ± 0.67 (CV 1.71%). The a^* values of the simulated PWS lesion on the human subject with normal skin were higher than those from the mannequin head model.

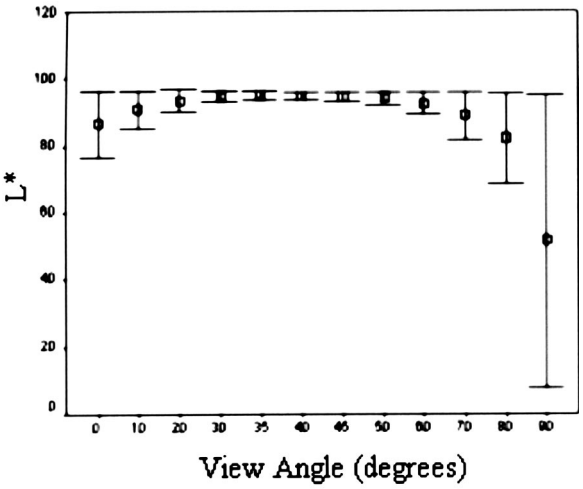

Fig. 6 Example illustrating the dependence of L^* values on view angle. In this measurement, patches 2 to 21 comprised the ROI, and the optimal view angle was determined to be 40 deg (CV=1.2%).

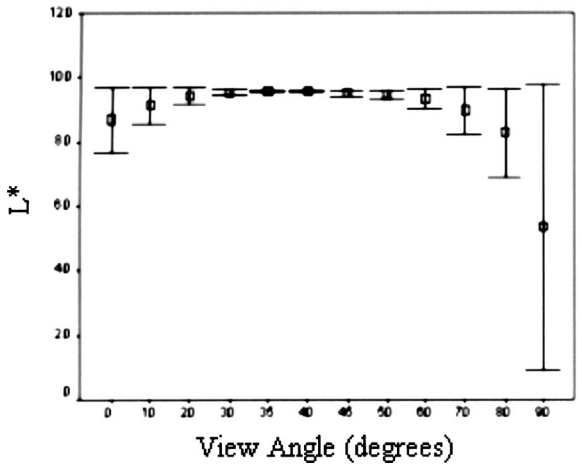

Fig. 7 Effect of view angle on L^* in the white patch ROI corresponding to the PWS-simulating red patches on the mannequin head model. The white patches numbers corresponding to the red patches were 2 to 9, 11 to 12, 14 to 16, 19 to 20, 23 to 24, and 27. The optimal view angle was 35 deg with a CV of 0.4% (μ, 95.87 and σ, $\pm$0.4).

3.3 *View Angle Affects the Quantitative Assessment of PWS Skin Erythema*

At the same PWS patient visit, two cross-polarized diffuse reflectance images were obtained at view angles of 20 deg (Fig. 8, top left) and 40 deg (Fig. 8, bottom left) and the corresponding a^* images computed (Fig. 8, top and bottom right, respectively). In comparing the two images, the region enclosed by the black line illustrated different a^* distributions as compared to the rest of the PWS lesion.

Using the CV-based analysis described, the optimal view angle to image the PWS lesion was determined to be 45 deg. Over an 8-week period, three cross-polarized diffuse reflectance color images were obtained from the same patient (Fig. 9, left side) at the optimal view angle of 45 deg. Qualitatively, it appears that while normal area presents quasiconstant skin color, red skin color in PWS lesion was gradually lighter in successive images due to the positive laser treatment effect. The changes of erythema seen in the images was emphasized in the corresponding quantitative a^* images (Fig. 9, right side). In the color bar, a higher a^* value means higher erythema.

4 Discussion

Our results indicate that view angle and facial curvature affect quantitative measurement of facial skin erythema. The distributions of reflected light from a 99% diffuse reflectance standard acquired at two view angles demonstrated that view angle affects the uniformity of the incident light distribution (Fig. 5). The flat reflectance standard is larger than the field of view of the camera at the working distance used in this study. At an optimal view angle (0 deg), at which the axis of the camera is perpendicular to the surface of the reflectance standard, the working distance is spatially constant on the flat surface and results in uniform light distribution [Fig. 5(a)]. However, at a suboptimal view angle of 35 deg, the working distance varies spatially, resulting in displacement of a portion of the reflectance standard away from the camera and lighting system, and displacement of a portion of the standard toward the camera and lighting system [Fig. 5(b)]. Since the exposure time and aperture for this set of experiments remained fixed, translation of the reflectance standard toward the camera and illumination system resulted in saturation of a portion of the sensing element (blooming). Note, however, that the graded decrease in illumination on the left portion of this image represents a 4% (or whatever it is) decrease in intensity. The apparent severity in the recorded illumination intensity is partially an artifact of the color scale that was chosen to make the effects of the angular offset readily apparent.

Table 1 Summary of optimal view angles for imaging different ROIs of the mannequin head model (Fig. 2).

Patch Location Numbers	Optimal View Angle (deg)	CV (%)
1 to 50	40	2.86
2 to 42	50	1.97
2 to 21	40	1.2
19 to 42	70	0.3

The variation in CV with view angle showed that an optimal view angle exists for a given facial surface curvature and ROI (Figs. 6 and 7). In the presented examples (Figs. 6 and 7), variations in CV are relatively insensitive to view angles of $\pm$10 deg from the determined optimal view angle. However, in clinical practice, it is obvious that reproducing head position at each patient visit is essential.

Evidence that view angle affects quantitative image analysis is that images acquired from the same subject at two different view angles possessed noticeable difference in a^* values on the higher facial curvature region compared to the relatively flat region (Fig. 8). This is due primarily to the difference in incident light distribution with view angle (Fig. 5). In evaluation of skin color at different patient visits, if the view angle is not optimized and held constant, quantitative

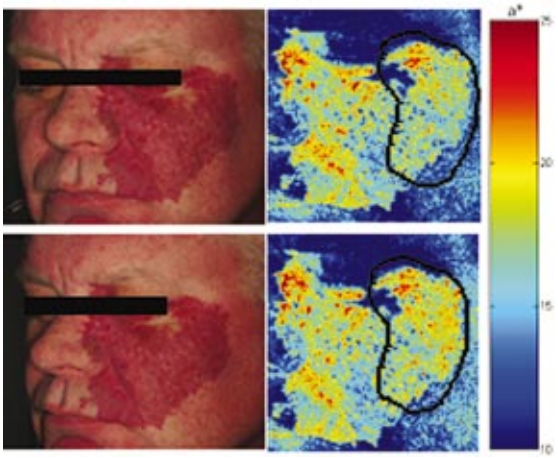

Fig. 8 Cross-polarized diffuse reflectance color (left) and *a** (right) images taken at view angles of 20 deg (top) and 40 deg (bottom). Angular artifact in quantitative assessment of *a** was emphasized in the ROI enclosed in the solid black line, in which *a** value distributions were different.

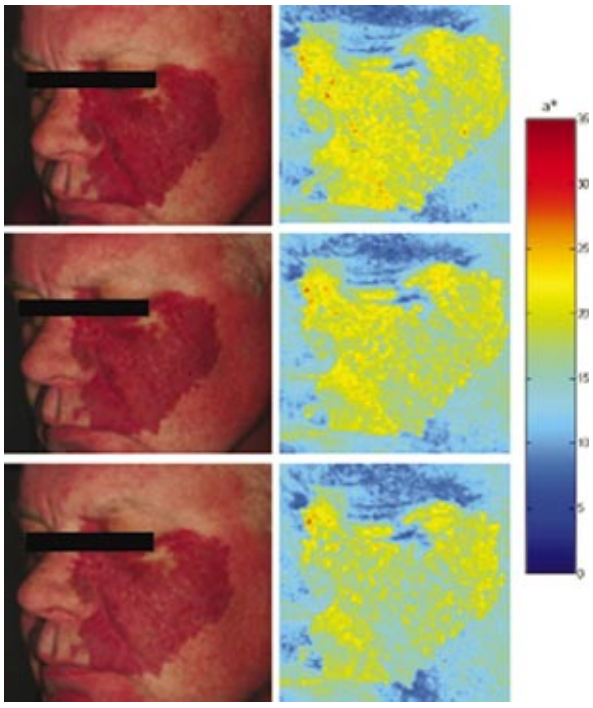

Fig. 9 Cross-polarized diffuse reflectance color images (left) and *a** images (right) of a PWS patient taken at the optimal view angle of 45 deg. The images were acquired at three successive visits over an 8-week period. The images from top to bottom indicate the first, second, and third visits, respectively. The image acquisition based on the optimal view angle provides comparable qualitative skin color images and enables us to use an absolute *a** image for quantitative assessment of response to laser treatment of PWS.

comparison of color changes in different ROIs is hindered by artifacts caused by differences in incident light distribution.

A surprising finding was that the mean a^* values of the simulated PWS birthmark on the human subject was higher than that from the mannequin head model. We expected the mean a^* values to be the same due to the use of identical red patches in both measurements. We believe that this discrepancy is due to differences in vertical tilt between the human subject and mannequin head model and to slight differences in placement of the red patches. In a separate experiment, red patches were placed on a flat panel, and the vertical tilt was changed from 0 to 10 deg. Resultant a^* values determined from the cross-polarized diffuse reflectance images were slightly different (38.5 versus 40.2 at 0 and 10 deg, respectively). Therefore, to maximize the accuracy of quantitative analysis determined from cross-polarized diffuse reflectance images, it is necessary to use a head-positioning device with adjustments for both vertical and horizontal tilt. We are currently working on the design of such a device.

Results obtained with the mannequin head model (Fig. 6) and human subjects with normal (Fig. 7) and PWS skin (Fig. 8) demonstrate the importance of considering the ROI in facial imaging. As shown in Table 1, the optimal view angle depends on the ROI. Furthermore, the CV was higher when a relatively large ROI was selected (e.g., patches 1 to 50) as compared to when a smaller ROI was considered; this results was due to the higher degree of nonuniformity in the illumination over the larger ROI due to local differences in facial curvature. This result is similar to that obtained by Miyamoto et al., who determined that when a ROI was close to the region used for color calibration, the error was minimized.[18] Therefore, we recommend that facial imaging should be performed at multiple view angles, and the optimal view angle determined individually for different ROIs. This recommendation enables direct quantitative comparison of images obtained at different patient visits to monitor the progress of PWS laser therapy throughout an extended treatment protocol (Fig. 9).

Currently, we are developing a program for clinicians to determine easily the optimal view angle in daily practice. In the program, clinicians determine the specific ROI of a patient and easily select the matched specific white patch numbers from the digitized mannequin head model, and finally, the optimal view angle is automatically determined with the selected white patches. In summary, we believe the approach described here can be applied to other color-based studies in which analog or digital imaging is employed.

Acknowledgments

The authors would like to acknowledge the Arnold and Mabel Beckman Fellows Program (BC), the National Institutes of Health/National Center for Research Resources (NIH/NCRR) Laser and Medical Microbeam Program (RR01192 AJD), and National Institutes of Health (AR47551, AR48458 and GM62177 JSN) for providing research grant support.

References

1. P. Clarys, K. Alewaeters, R. Lambrecht, and A. O. Barel, ''Skin color measurements: comparison between three instruments: the chromameter, the dermaspectrometer and the mexameter,'' *Skin Res. Technol.* **6**, 230–238 (2000).
2. M. D. Shriver and E. Parra, ''Comparison of narrow-band reflectance spectroscopy and tristimulus colorimetry of measurements of skin and hair color in persons of different biological ancestry,'' *Am. J. Phys. Anthropol.* **112**, 17–27 (2000).
3. A. M. Trolius and B. Ljungren, ''Evaluation of port wine stains by laser Doppler perfusion imaging and reflectance photometry before and after pulsed dye laser treatment,'' *Acta Derm Venereol* **76**, 291–294 (1996).
4. E. Berardesca, P. Elsner, and H. I. Maibach, *Bioengineering of The skin: Cutaneous Blood Flow and Erythema*, pp. 60–63, CRC Press, Boca Raton, FL (1995).
5. A. M. Trolius and B. Ljungren, ''Reflectance spectrophotometry in the objective assessment of dye laser-treated port-wine stains,'' *Br. J. Dermatol.* **132**, 245–250 (1995).
6. H. Takiwaki, Y. Miyaoka, H. Kohno, and S. Arase, ''Graphic analysis of the relationship between skin colour change and variations in the amounts of melanin and hemoglobin,'' *Skin Res. Technol.* **8**, 78–83 (2002).
7. M. Seraro and A. Sparavigna, ''Quantification of erythema using digital camera and computer-based image analysis: a multicentre study,'' *Skin Res. Technol.* **8**, 84–88 (2002).
8. K. Miyamoto, H. Takiwaki, G. G. Hillebrand, and S. Arase, ''Development of a digital imaging system for objective measurement of hyperpigmented spots on the face,'' *Skin Res. Technol.* **8**, 227–235 (2002).
9. S. A. Young-Gee, H. A. Kurwa, and R. J. Barlow, ''Objective assessment of port-wine stains following treatment with the 585 nm pulsed dye laser,'' *Australas J. Dermatol.* **42**, 243–246 (2001).
10. D. K. Rah, S. H. Kim, K. H. Lee, B. Y. Park, and D. W. Kim, ''Objective evaluation of treatment effects on port-wine stains using $L^*a^*b^*$ color coordinate,'' *Plast. Reconstr. Surg.* **108**, 842–847 (2001).
11. A. Fullerton, T. Fischer, A. Lahti, K.-P. Wilhelm, H. Takiwaki, and J. Serup, ''Guidelines for measurement of skin colour and erythema,'' *Contact Dermatitis* **35**, 1–10 (1996).
12. B. Jung, B. Choi, A. J. Durkin, K. M. Kelly, and J. S. Nelson, ''Characterization of port wine stain skin erythema and melanin content using cross-polarized diffuse reflectance imaging,'' *Lasers Surg. Med.* **34**, 174–181 (2004).
13. S. L. Jacques, J. R. Roman, and K. Lee, ''Imaging superficial tissues with polarized light,'' *Lasers Surg. Med.* **26**, 119–129 (2000).
14. A. J. Welch and M. J. C. van Gemert, *Optical-Thermal Response of Laser-Irradiated Tissue, Plenum Press*, New York (1995).
15. D. Malacara, *Color Vision and Colorimetry: Theory and Applications*, pp. 90–101, SPIE Press, Bellingham, WA (2002).
16. Y. V. Haeghen, J. M. D. N. Naeyaert, and I. Lemahieu, ''An imaging system with calibrated color image acquisition for use in dermatology,'' *IEEE Trans. Med. Imaging* **19**, 722–730 (2000).
17. W. Alaluf, D. Atkins, K. Barrett, M. Blount, N. Carter, and A. Heath, ''The impact of epidermal melanin on objective measurements of human skin color,'' *Pigment Cell Res.* **15**, 119–126 (2002).
18. K. Miyamoto, H. Takiwaki, G. G. Hillebrand, and S. Arase, ''Utilization of a high-resolution digital imaging system for the objective and quantitative assessment of hyperpigmented spots on the face,'' *Skin Res. Technol.* **8**, 73–77 (2002).